OPEN

Comparison of the Timing of Hepatic Arterial Phase and Image Quality Using Test-Bolus and Bolus-Tracking Techniques in Gadolinium–Ethoxybenzyl–Diethylenetriamine Pentaacetic Acid–Enhanced Hepatic Dynamic Magnetic Resonance Imaging

Yuji Iyama, MD,† Takeshi Nakaura, PhD,† Koichi Yokoyama, MD,*† Masafumi Kidoh, PhD,† Daisuke Utsunomiya, PhD,† Seitaro Oda, PhD,† Tomohiro Namimoto, PhD,† and Yasuyuki Yamashita, PhD†*

Objectives: The aim of this study was to compare the image quality, the degree of artifacts and the percentage of timing of the optimal hepatic arterial phase (HAP) between test-bolus and bolus-tracking methods on gadolinium–ethoxybenzyl–diethylenetriamine pentaacetic acid (Gd-EOB-DTPA)–enhanced magnetic resonance imaging (MRI).

Methods: In this prospective study, 60 patients who underwent 3-dimensional dynamic Gd-EOB-DTPA–enhanced hepatic 3-T MRI were enrolled in this study. We randomly assigned the 30 patients to the bolus-tracking method, and another 30 patients to the test-bolus method. Signal-to-noise ratios of the liver and spleen in HAP were compared in the 2 groups. Two radiologists independently assessed the ratio of optimal timing of HAP and the degree of ringing and motion artifacts of the 2 protocols.

Results: The signal-to-noise ratios of the liver (24.0 [SD, 6.4] vs 20.4 [SD, 4.0]) and spleen (30.0 [SD, 13.3] vs 23.6 [SD, 9.9]) were significantly higher in the test-bolus protocol than in the bolus-tracking protocol. The ratio of optimal timing was also significantly higher with the test-bolus protocol than with the bolus-tracking protocol (76.7% vs 40.0%). The degree of ringing and motion artifacts of test-bolus protocol was significantly lower than that of the bolus-tracking protocol ($P < 0.01$).

Conclusions: The test-bolus protocol in dynamic 3-T MRI can yield better qualitative image quality and more optimal timing of HAP images, while reducing the degree of artifacts compared with the bolus-tracking protocol.

Key Words: gadolinium-ethoxybenzyl-DTPA, imaging, liver, magnetic resonance imaging, techniques

(*J Comput Assist Tomogr* 2017;41: 638–643)

Hepatic dynamic magnetic resonance imaging (MRI) has been reported to have high diagnostic performance for benign, malignant, hypervascular, and hypovascular tumors and metastatic liver tumors.[1–3] The introduction of gadolinium–ethoxybenzyl–diethylenetriamine pentaacetic acid (Gd-EOB-DTPA) for clinical use has enabled the evaluation of tumor vascularity and hepatic function on single Gd-EOB-DTPA–enhanced MRI examinations.[4,5] The timing of hepatic arterial phase (HAP) is an integral component of dynamic MRI to distinguish benign from malignant hypervascular tumor.[6] The fixed timing method of dynamic hepatic MRI has been reported to result in suboptimal timing of HAP images in many patients.[1,7] Optimal HAP timing with Gd-EOB-DTPA is actually more difficult than with Gd-DTPA because of the halved injected volume of Gd-EOB-DTPA. Initial clinical trials considered that the injection of a 0.0125-mmol/kgc dose was sufficient; the standard dose applied and recommended by recent studies is 0.025 mmol/kgc, because of a better delimitation of focal lesions and improvement of the contrast-to-noise ratio.[8] Previous study suggested that slower injection rate of Gd-EOB-DTPA (1 mL/s) technique can yield a higher enhancement in aorta in HAP compared with the conventional injection rate of Gd-EOB-DTPA (2 mL/s) technique in hepatic dynamic MRI.[9] The reason was that the longer injection time allows a broader arterial peak, with fewer problems in arterial phase acquisition.

Test-bolus and bolus-tracking methods have been widely used to determine the time to start scanning.[10,11] The test-bolus method was reported to result in more optimal HAP timing than the fixed-time method.[10,12,13] To date, however, no reports have compared image quality of the test-bolus and bolus-tracking methods in patients undergoing dynamic liver enhanced 3-T MRI. This study was designed to compare qualitative image quality, the degree of artifacts, and the optimal timing of the HAP using test-bolus and real-time bolus-tracking methods in patients undergoing Gd-EOB-DTPA–enhanced MRI.

MATERIALS AND METHODS

This prospective study was approved by our institutional review board, and informed written consent was obtained from all patients prior to their participation in this study.

Patients

Between October 2012 and April 2013, 60 consecutive patients in our institution underwent dynamic MRI of the liver. Of these, 30 patients (19 men and 11 women; mean age, 71.3 [SD, 7.8]years; body weight range, 40–75 kg; median body weight, 55.6 kg) were randomized by using random table to undergo scanning with Gd-EOB-DTPA–enhanced MRI using the bolus-tracking method, whereas the other 30 patients (18 men and 12 women; mean age, 70.8 [SD, 11.5]years; body weight range, 45–83 kg; median body weight, 57.9 kg) underwent scanning with Gd-EOB-DTPA–enhanced MRI using the test-bolus method. Patients having or suspected of having hepatocellular carcinoma (HCC) were included in this study. The exclusion criterion was

From the *Diagnostic Radiology, Amakusa Medical Center; and †Department of Diagnostic Radiology, Graduate School of Medical, Kumamoto University, Amakusa, Japan.

Received for publication August 24, 2016; accepted October 24, 2016.

Correspondence to: Yuji Iyama MD, Diagnostic Radiology, Amakusa Medical Center, Kameba 854-1, Amakusa, Kumamoto 863-0046, Japan (e-mail: iyamayuuji28@gmail.com).

The authors declare no conflict of interest.

DOI: 10.1097/RCT.0000000000000583

severe renal dysfunction (estimated glomerular filtration rate, <30 mL/min per 1.73 m^2). No patients were excluded from this study. There were 2 patients who were scanned with both the bolus-tracking method and the test-bolus method.

MRI Protocol

All patients underwent dynamic, ultrafast, T1-weighted, 3-dimensional (3D) turbo-gradient-echo (GRE) sequence with fat suppression (mDixon-3D-GRE sequence) on a 3-T scanner (Ingenia; Philips Medical Systems, Best, The Netherlands) and were injected with 0.025 mmol/kg (0.1 mL/kg) of Gd-EOB-DTPA at a rate of 2 mL/s, followed by injection of 20 mL saline at 2 mL/s using a power injector. The patients held their breath in end expiration. Table 1 describes the sequences and parameters of mDixon-3D-GRE sequence with the bolus-tracking and test-bolus protocols. Images from both protocols were acquired in the transverse plane, with a reception time (TR)/echo time (TE) ratio of 3.50/TE1, 1.26; TE2, 2.20. The flip angle was 15 degrees, the number of acquisitions was 1, the field of view (FOV) was 350 × 278 mm, the matrix was 232 × 139, and the acquisition time was 13.5 seconds.

The bolus-tracking protocol for arterial-phase imaging consisted of 4 sequential elements. First, real-time bolus monitoring was concurrent with contrast administration. Second, the radiology technologist stopped bolus tracking when contrast was visualized in the abdominal aorta at the level of the celiac axis (diaphragm). Third, patients held their breath. Fourth, breath-hold 3D-GRE sequence was acquired. Real-time bolus-track imaging was implemented using a 2-dimensional GRE sequence, with acquisitions every 0.939 second and on-the-fly image reconstruction (FOV, 500 × 500 mm; matrix, 256 × 128; TR/TE/flip angle, 7.3/3.1 milliseconds/40 degrees; slice thickness, 80 mm). The sequence was oriented in the coronal plane, along the abdominal aorta, and initiated at the same time as contrast administration. Real-time images were displayed on the console using an inline viewer. A manual pause of 6 to 7 seconds was implemented after cessation of the bolus-tracking sequence, during which breath-holding instructions were given to the patient before initiating 3D-GRE sequence. The duration of the pause was optimized based on the results of perfusion data acquired in this study and the approximate center of the k-space within the 3D-GRE technique. Arterial-phase images were obtained using a 3D-GRE imaging sequence with a segmented k-space acquisition. The estimated time to the center of k-space was 4.6 seconds, ensuring the initial part of the scan effectively coincides with the collection of the desired image contrast. Both protocols acquired k-space data linearly over many segments.

TABLE 1. MRI Sequence and Parameters

Sequence	Bolus-Tracking and Test-Bolus Protocols
TR, ms	3.5
TE, ms	TE1, 1.23; TE2, 2.2
Slice thickness, mm	1.5
FA, degrees	10
Matrix	232 × 121
FOV, mm	350 × 278
No. of slices	150
Voxel size, mm^3	1.51 × 1.99 × 3.0
No. of acquisitions	1
Band width, Hz/pixel	1436.8
Mean acquisition time, s	12.6

FA indicates flip angle.

The test-bolus consisted of 0.125 mmol (0.5 mL) Gd-EOB-DTPA followed by the injection of 50 mL saline at 2 mL/s. Images were acquired in the transverse plane, with a TR/TE ratio of 3.50/TE1, 1.26; TE2, 2.20. The flip angle was 15 degrees, the number of acquisitions was 1, the FOV was 350 × 278 mm, and the matrix was 232 × 139. The purpose of this image was to visualize the abdominal aorta, not the tumor. A previous report suggested that optimal HAP timing was $T_{test\_peak} + T_{full\_bolus} + T_{tumor} - T_{k\_space}$.[11] T_{test_peak} was defined as the time to peak aortic enhancement from the start of test-bolus injection, T_{full_bolus} as the time delay from peak aortic enhancement of the test bolus to peak aortic enhancement of the full bolus, T_{tumor} as the time delay from peak aortic to peak tumor enhancement, and T_{k_space} as the time to the center of the k-space acquisition. Previous report suggested that T_{full_bolus} was equal to half of the contrast injection duration by evaluating the abdominal aorta of pig.[14] In addition, we have defined the T_{tumor} as 8 seconds referenced with previous report.[11] Therefore, the optimal HAP was assumed to be $T_{test\_peak} + T_{full\_bolus} + T_{tumor} - T_{k\_space} = T_{test\_peak}$ + (half of the contrast injection duration) + 8 − T_{k_space}.[11] Optimal HAP timing for the test-bolus protocol was also defined using the above equation. Using both protocols, portal venous phase and venous phase images were acquired 30 and 150 seconds, respectively, after HAP.

Quantitative Image Analysis

All quantitative image analyses were performed by 1 radiologist, with 5 years of experience in abdominal imaging, who was blinded to the study protocol. Operator-defined regions of interest were measured on the HAP. The mean signal intensity of the normal hepatic parenchyma of the left and right lobes at the level of the root of the celiac trunk was obtained from 2 circular areas of diameter approximately 20 mm, avoiding tumors, large vessels, dilated biliary ducts, and prominent artifacts. If a patient had previously undergone a lobectomy of the liver, the mean signal intensity was measured by 2 circular areas of the remaining liver. The mean signal intensity of the spleen of the upper and lower poles was obtained from 2 circular areas of diameter approximately 10 mm avoiding large vessels and prominent artifacts. The signal-to-noise ratios (SNRs) of the liver and spleen were calculated by dividing image noise. Image noise was measured in the SD of air outside the patient's body avoiding phase artifacts.

We also performed post hoc power ($1 - \beta$) analysis between the groups using standardized mean differences and sample size and α (1-tailed) level of 0.05 with G*Power software (version 3.1.3; Faul and Erdfelder, University of Düsseldorf, Düsseldorf, Germany) in quantitative analysis.

Qualitative Analysis

Scan timing and image quality, including the degree of artifacts, were evaluated qualitatively by 2 independent readers, who had 5 and 8 years of experience, respectively, with abdominal MRI. The MRI data sets of the 60 patients were randomized, and the radiologists were blinded to the injection methods and all patient data.

Scan timing was evaluated using enhancement of the renal, splenic, portal, superior mesenteric, and hepatic veins as landmarks and a 5-point scale, in which 1 (too early) indicated that the major part of the renal vein was not opacified; 2 (very early), that the renal vein was completely opacified, but the major part of the splenic vein was not opacified; 3 (good), that the major part of the splenic vein was opacified, but the portal vein was only partially opacified; 4 (late-good), that the major part of the portal vein was opacified, but the hepatic vein was not opacified; and 5 (too late), that the hepatic vein was opacified. Images with scores of 3 and 4 were defined as optimal, and the frequency of optimal

HAP images was compared for the 2 protocols. Second, the degree of ringing and motion artifacts on HAP images were evaluated using a 4-point scale (excellent, good, poor, and nondiagnostic) to grade image quality. On this scale, 4 (excellent) was defined as absence of artifacts, 3 (good) as a slight ringing or motion artifact that did not interfere with the diagnosis, 2 (poor) as an artifact interfering with the diagnosis, and 1 (nondiagnostic) as an obvious artifact rendering image assessment almost impossible. By definition, ringing artifacts are centered on the vessels and confined to the abdomen, whereas respiratory motion artifacts are centered on the abdominal wall and can extend outside it.

Examples of these artifacts are shown in Figure 1. In cases of interobserver disagreement, they discussed and reached consensus. The degree of interobserver agreement for each qualitative assessment was determined by calculating the κ value.

Statistical Analysis

We compared SNR of liver and spleen between 2 protocols, using unpaired *t* test. The frequency of optimal HAP images using the 2 protocols was compared using the χ^2 test, and the degree of artifacts was compared using the Mann-Whitney *U* test. Probability values of less than 0.05 were considered statistically significant. κ Coefficients for interobserver agreement of less than 0.20, 0.21 to 0.40, 0.41 to 0.60, 0.61 to 0.80, and 0.81 to 1.00 were defined as poor, fair, moderate, substantial, and nearly perfect, respectively. All statistical analyses were performed with R, version 2.6.1 software (The R Project for Statistical Computing; http://www.r-project.org/).

RESULTS

The 2 groups were well matched in age ($P = 0.84$), sex distribution ($P = 0.88$), and BW ($P = 0.35$) (Table 2).

Quantitative Analysis

Table 3 shows the SNRs of the liver and spleen determined by the 2 protocols. Signal-to-noise ratios of the liver (24.0 [SD, 6.4] vs 20.4 [SD, 4.0], $P < 0.05$) and spleen (30.0 [SD, 13.3] vs 23.6 [SD, 9.9], $P < 0.05$) on HAP images were significantly higher using the test-bolus protocol than using the bolus-tracking protocol. The test powers for SNR of each ROI were 70.2% for liver and 54.2% for spleen.

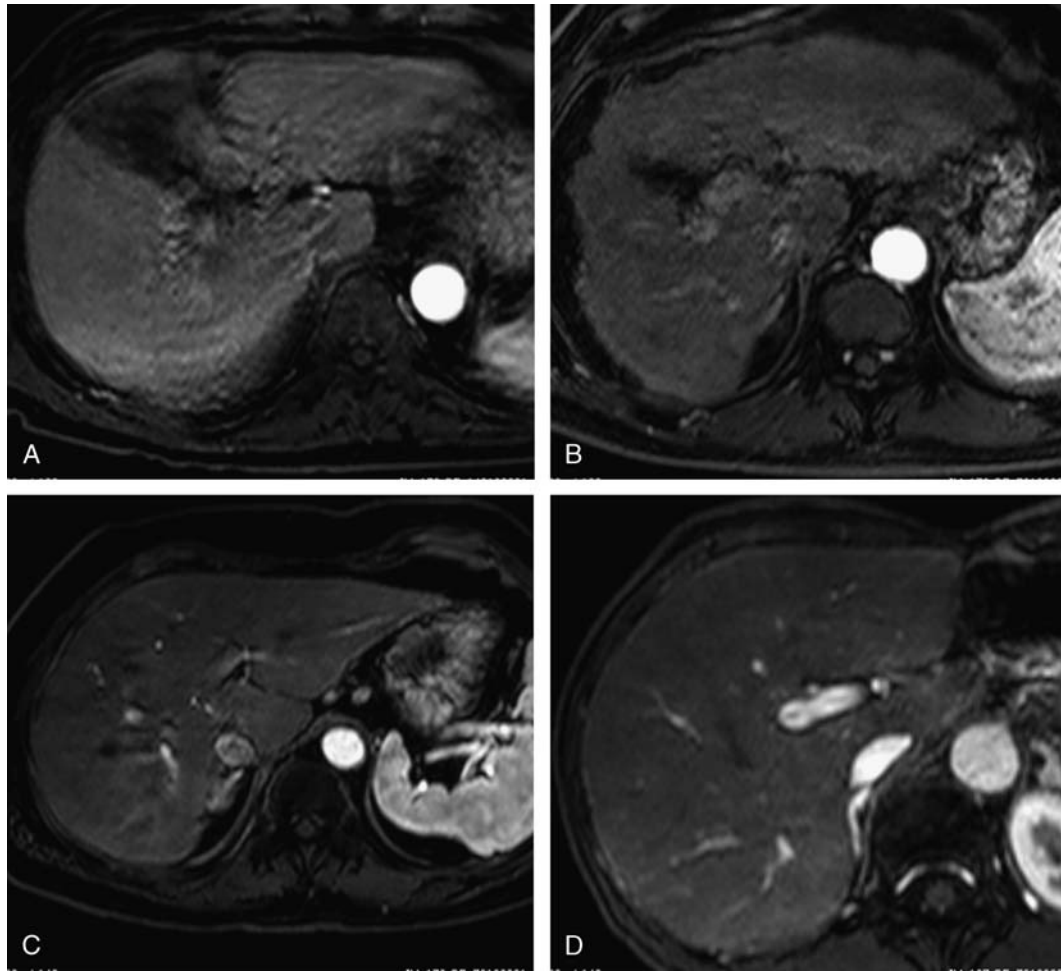

FIGURE 1. Examples of image quality assessed using a 4-point scale (excellent, good, poor, and nondiagnostic). A, Nondiagnostic: the ringing and motion artifact was obvious, and rendered image assessment almost impossible. B, Poor: the ringing artifact interfered with the diagnosis. C, Good: a slight ringing or motion artifact was observed, but it did not interfere with the diagnosis. D, Excellent: no artifact was observed.

TABLE 2. Baseline Demographic and Clinical Characteristics

	Bolus-Tracking Protocol	Test-Bolus Protocol	*P*
No. of patients	30	30	
Mean (SD) age, y	71.3 (7.9)	70.8 (11.5)	0.84
No. of male/female patients	18/12	19/11	0.88
Mean (SD) body weight, kg	58.0 (8.6)	55.6 (10.7)	0.35

Qualitative Analysis

Visual scores assessing the degree of ringing and motion artifacts were significantly higher using the test-bolus than the bolus-tracking protocol (ringing artifact, 3.6 [SD, 0.5] vs 3.0 [SD, 0.9] [$P < 0.05$]; motion artifact, 3.7 [SD, 0.4] vs 3.1 [SD, 1.1] [$P < 0.05$]). Interobserver agreement was substantial to nearly perfect, respectively ($\kappa = 0.69$ and 0.85).

Table 4 also shows visual scores about the timing of HAP. The proportion of scans yielding optimal HAP (scores of 3 and 4) was significantly higher using the test-bolus than the bolus-tracking protocol, as determined by both reader 1 (76.7% [23/30] vs 40.0% [12/30], $P < 0.01$) and reader 2 (73.3% [22/30] vs 36.4% [11/30], $P < 0.01$). Interobserver agreement was substantial ($\kappa = 0.67$). Representative scans are shown in Figures 2 and 3.

DISCUSSION

This study showed that the test-bolus method was superior to the bolus-tracking method of Gd-EOB-DTPA–enhanced hepatic dynamic MRI in producing optimally timed images and higher SNR and lower degree of artifact images. Hepatic arterial phase images obtained with the bolus-tracking protocol tend to be suboptimal, because breath hold and scanning were started manually only after abdominal aortic enhancement was ascertained. As the delays in breath hold and peak contrast enhancement of the liver vary, scanning at optimal HAP time may not be possible. The bolus-tracking method is simpler and faster to perform than the test-bolus method.[1] However, the delay in optimal HAP scan timing may be critical for dynamic MRI; because the total amount of Gd-EOB is much smaller than that of Gd. The smaller amount of contrast medium reduces the peak contrast enhancement by Gd-EOB-DTPA, as well as the time to peak contrast enhancement, resulting in more accurate peak contrast enhancement timing than with Gd-DTPA. Thus, in this study, the test-bolus protocol was more suited for dynamic MRI than the bolus-tracking protocol.

Our study also suggested that the test-bolus method can yield higher SNR images compared with bolus-tracking method. The reason might be that test-bolus method can scan at more optimal timing at HAP compared with bolus-tracking method. At optimal timing, HAP and high-concentration gadolinium chelates produced a significantly increased maximum signal change and resulted in an improved SNR.

In addition, our study suggested that the test-bolus technique reduces the degree of ringing and motion artifacts during imaging compared with the bolus-tracking method. Preserving the homogeneity of k-space data acquisition and reducing truncation and ringing artifacts are critical for dynamic MRI.[15] Ringing artifacts are derived truncation artifacts in a narrow sense and include phase ghosts from organs and blood vessels. The center of k-space contains the low spatial frequencies and contrast information of each image. A marked alteration in gadolinium concentration around the center of k-space during acquisition in arterial phase produces ringing artifacts.[16,17] These phenomena are dependent on scan timing and the injection method.[15,18,19] The lower number of artifacts observed using the test-bolus protocol may be due to the ability of this protocol to provide a more exact time of peak enhancement than the bolus-tracking protocol.

Moreover, we supposed that the respiratory motion artifact in test-bolus protocol might be less than that in bolus-tracking protocol. The radiology technologist can expect the starting breath-holding time is more accurate in test-bolus protocol than that in bolus-tracking protocol. Therefore, breath-holding time might be less in test-bolus protocol than that in bolus-tracking protocol. The shortening of breath-holding time is important to scan optimal HAP image without breath motion artifact. The reason was that the radiology technologist can get the time density curve by test contrast injection. Therefore, the motion artifact in test-bolus protocol was less than that in bolus-tracking protocol in this study. Indeed, previous report suggested that the use of single-breath-hold, multiple-arterial-phase acquisition technique can yield inconspicuous motion artifact HAP images by shortening acquisition time and breath-holding time during single acquisition time.[20]

This study had several limitations. First, this study with an insufficient sample size did not have sufficient statistical power to verify our end points. Although confirmation requires evaluation of more patients, this is offset by our results showing that patients benefit from the test-bolus protocol. Second, between-group differences in some factors, such as cardiovascular function, body habitus, and body fat and the presence of cirrhosis or portal hypertension or fatty liver, may have influenced the study results.[20] Third, we did not compare these 2 methods in the diagnosis of HCC, indicating the need for additional studies to determine which, if any, technique is superior in the diagnosis of HCC. Fourth, although respiratory motions have been reported to be more responsible for the truncation artifacts in arterial phase in Gd-EOB-DTPA–enhanced MRI than in Gd-DTPA–enhanced MRI,[21] this study did not evaluate the effects of respiratory motion artifacts in the arterial phase. Lastly, we did not use the lower injection of Gd-EOB-DTPA technique (1 mL/s). Previous study suggested that the lower injection technique was better to scan optimal HAP timing compared with the conventional injection technique (2 mL/s). In addition, we did not compare with multiphase imaging in this study. Previous report suggested that triple arterial acquisition method can yield optimal HAP timing

TABLE 3. Quantitative Image Analysis

	Bolus-Tracking Protocol	Test-Bolus Protocol	*P*
SNR Liver	20.4 (4.0)	24.0 (6.4)	<0.05
Spleen	23.6 (9.9)	30.0 (13.3)	<0.05

Data are shown as mean (SD).

TABLE 4. Qualitative Image Analysis (Interobserver Agreements)

	Bolus-Tracking Protocol	Test-Bolus Protocol	*P*
Degree of ringing artifacts	3.0 (0.9)	3.6 (0.5)	<0.05
Degree of motion artifacts	3.1 (1.1)	3.7 (0.4)	<0.05
Ratio of optimal HAP	40.0%	76.7%	<0.05

The distribution of patients about the timing of HAP between bolus-tracking protocol and test-bolus protocol (interobserver agreement). The proportion of scans yielding optimal HAP (scores of 3 and 4) was significantly higher using the test-bolus than the bolus-tracking protocol (76.7% [23/30] vs 40.0% [12/30], $P < 0.0$).

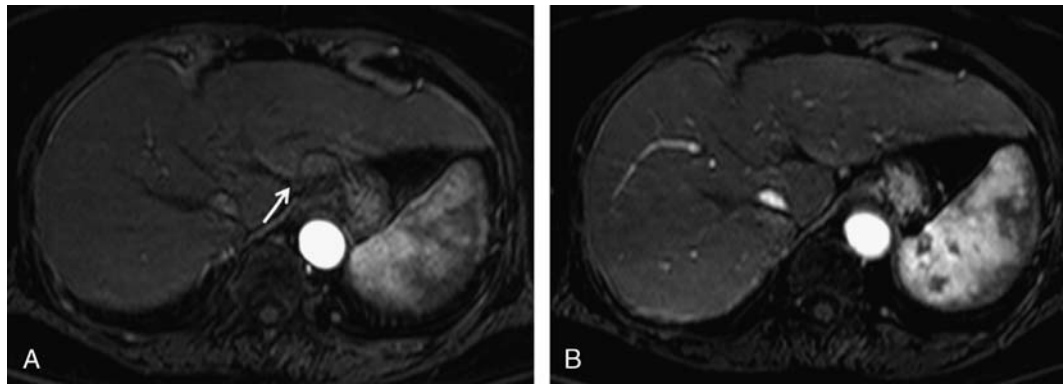

FIGURE 2. A 78-year-old woman with chronic liver disease caused by hepatitis C virus infection, who was scanned with the bolus-tracking and test-bolus protocols. A, A slight artifact (arrow) was observed in the HAP image with the bolus-tracking method. B, This artifact was inconspicuous in the HAP image with the test-bolus method.

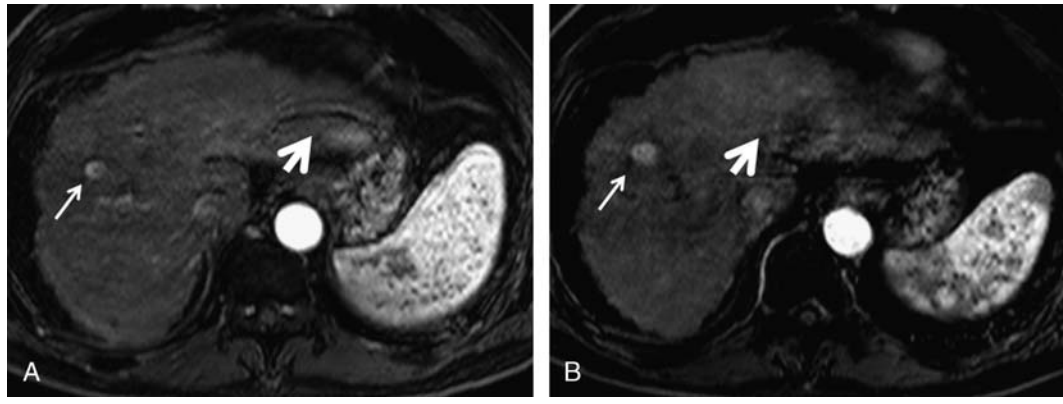

FIGURE 3. A 63-year-old man with chronic liver disease caused by hepatitis C virus infection and HCC, who was scanned with the bolus-tracking and test-bolus protocols. A, A 3D T1-weighted GRE sequence with fat-suppression image, clearly showing a hypervascular HCC (thick arrow), as well as a slight artifact (thin arrow) in the HAP image with the bolus-tracking method. B, This artifact is inconspicuous in the HAP image with the test-bolus method.

images more frequently than fixed time method.[22] Therefore, we would compare test-bolus protocol, bolus-tracking protocol, fixed time method, and multiphase imaging method in artifact and frequency of optimal timing of HAP using lower injection technique in a future study. Lastly, the small amount of contrast in test bolus might affect the image quality. However, the contrast of test bolus is too small to affect the image quality in the arterial phase, because the test bolus has been greatly diluted in the extracellular fluid volume.

In conclusion, compared with the bolus-tracking protocol, the test-bolus protocol in Gd-EOB-DTPA–enhanced 3-T MRI can yield better qualitative image quality and more optimal timing of HAP, as well as reducing the degree of artifacts.

REFERENCES

1. Earls JP, Rofsky NM, DeCorato DR, et al. Hepatic arterial-phase dynamic gadolinium-enhanced MR imaging: optimization with a test examination and a power injector. *Radiology*. 1997;202:268–273.
2. Kanematsu M, Semelka RC, Matsuo M, et al. Gadolinium-enhanced MR imaging of the liver: optimizing imaging delay for hepatic arterial and portal venous phases—a prospective randomized study in patients with chronic liver damage. *Radiology*. 2002;225:407–415.
3. Brown ED, Semelka RC. Contrast-enhanced magnetic resonance imaging of the abdomen. *Magn Reson Q*. 1994;10:97–124.
4. Frericks BB, Loddenkemper C, Huppertz A, et al. Qualitative and quantitative evaluation of hepatocellular carcinoma and cirrhotic liver enhancement using Gd-EOB-DTPA. *AJR Am J Roentgenol*. 2009;193:1053–1060.
5. Narita M, Hatano E, Arizono S, et al. Expression of OATP1B3 determines uptake of Gd-EOB-DTPA in hepatocellular carcinoma. *J Gastroenterol*. 2009;44:793–798.
6. Quillin SP, Atilla S, Brown JJ, et al. Characterization of focal hepatic masses by dynamic contrast-enhanced MR imaging: findings in 311 lesions. *Magn Reson Imaging*. 1997;15:275–285.
7. Shinozaki K, Yoshimitsu K, Irie H, et al. Comparison of test-injection method and fixed-time method for depiction of hepatocellular carcinoma using dynamic steady-state free precession magnetic resonance imaging. *J Comput Assist Tomogr*. 2004;28:628–634.
8. Reimer P, Rummeny EJ, Shamsi K, et al. Phase II clinical evaluation of Gd-EOB-DTPA: dose, safety aspects, and pulse sequence. *Radiology*. 1996;199:177–183.
9. Schmid-Tannwald C, Herrmann K, Oto A, et al. Optimization of the dynamic, Gd-EOB-DTPA–enhanced MRI of the liver: the effect of the injection rate. *Acta Radiol*. 2012;53:961–965.
10. Sharma P, Kalb B, Kitajima HD, et al. Optimization of single injection liver arterial phase gadolinium enhanced MRI using bolus track real-time imaging. *J Magn Reson Imaging*. 2011;33:110–118.
11. Nakamura S, Nakaura T, Kidoh M, et al. Timing of the hepatic arterial phase at Gd-EOB-DTPA–enhanced hepatic dynamic MRI: comparison

of the test-injection and the fixed-time delay method. *J Magn Reson Imaging*. 2013;38:548–554.

12. Chan R, Kumar G, Abdullah B, et al. Optimising the scan delay for arterial phase imaging of the liver using the bolus tracking technique. *Biomed Imaging Interv J*. 2011;7:e12.
13. Goshima S, Kanematsu M, Kondo H, et al. Optimal acquisition delay for dynamic contrast-enhanced MRI of hypervascular hepatocellular carcinoma. *AJR Am J Roentgenol*. 2009;192:686–692.
14. Bae KT, Heiken JP, Brink JA. Aortic and hepatic contrast medium enhancement at CT. Part II. Effect of reduced cardiac output in a porcine model. *Radiology*. 1998;207:657–662.
15. Tanimoto A, Higuchi N, Ueno A. Reduction of ringing artifacts in the arterial phase of gadoxetic acid–enhanced dynamic MR imaging. *Magn Reson Med Sci*. 2012;11:91–97.
16. Taber KH, Herrick RC, Weathers SW, et al. Pitfalls and artifacts encountered in clinical MR imaging of the spine. *Radiographics*. 1998;18:1499–1521.
17. Mirowitz SA, Lee JK, Gutierrez E, et al. Dynamic gadolinium-enhanced rapid acquisition spin-echo MR imaging of the liver. *Radiology*. 1991;179: 371–376.
18. Zech CJ, Vos B, Nordell A, et al. Vascular enhancement in early dynamic liver MR imaging in an animal model: comparison of two injection regimen and two different doses Gd-EOB-DTPA (gadoxetic acid) with standard Gd-DTPA. *Invest Radiol*. 2009;44:305–310.
19. Motosugi U, Ichikawa T, Sou H, et al. Dilution method of gadolinium ethoxybenzyl diethylenetriaminepentaacetic acid (Gd-EOB-DTPA)–enhanced magnetic resonance imaging (MRI). *J Magn Reson Imaging*. 2009;30:849–854.
20. Hussain HK, Londy FJ, Francis IR, et al. Hepatic arterial phase MR imaging with automated bolus-detection three-dimensional fast gradient-recalled-echo sequence: comparison with test-bolus method. *Radiology*. 2003;226:558–566.
21. Davenport MS, Viglianti BL, Al-Hawary MM, et al. Comparison of acute transient dyspnea after intravenous administration of gadoxetate disodium and gadobenate dimeglumine: effect on arterial phase image quality. *Radiology*. 2013;266:452–461.
22. Sofue K, Marin D, Jaffe TA, et al. Can combining triple-arterial phase acquisition with fluoroscopic triggering provide both optimal early and late hepatic arterial phase images during gadoxetic acid–enhanced MRI? *J Magn Reson Imaging*. 2016;43:1073–1081.